Studies on Analogues of Classical Antifolates Bearing the Naphthoyl Group in Place of Benzoyl in the Side Chain

James R. Piper,*,† Cheryl A. Johnson,† Joseph A. Maddry,† Neeta D. Malik,† John J. McGuire,‡ Glenys M. Otter,§ and Francis M. Sirotnak§

Organic Chemistry Research Department, Southern Research Institute, Birmingham, Alabama 35255, Grace Cancer Drug Center, Roswell Park Cancer Institute, Buffalo, New York 14263, and Memorial Sloan-Kettering Cancer Center, New York, New York 10021

Received July 26, 1993®

Analogues of classical antifolates with the 4-aminobenzoyl group replaced by 4-amino-1-naphthoyl were synthesized for study after molecular modeling indicated ample spatial accommodation for the naphthalene ring and even larger groups in models based on reported X-ray crystallographic data describing the binding of methotrexate to human dihydrofolate reductase (DHFR). The side-chain precursors, *N*-(4-amino- and 4-(methylamino)-1-naphthoyl)-L-glutamic acid diethyl esters, were synthesized, and the 2,4-diamino-substituted heterocyclic groups were attached using several methods. Target compounds included naphthoyl analogues of aminopterin (AMT), methotrexate (MTX), 5-deazaAMT, 5-deazaMTX, 5-methyl-5-deazaAMT, 5-methyl-5-deazaMTX, and 5,8-dideazaAMT. A 5,6,7,8-tetrahydronaphthoyl analogue of 5-deazaAMT was also prepared. None of the naphthoyl analogues showed loss in binding to DHFR compared with the corresponding antifolate bearing the benzoyl group, thus confirming the anticipated bulk tolerance. Only the 5,6,7,8-tetrahydronaphthoyl analogue displayed reduced antifolate effects. Substrate activity toward folylpolyglutamate synthetase was, however, severely compromised. The naphthoyl compounds were transported into L1210 cells 3–6 times more readily than MTX, and despite apparently low levels of intracellular polyglutamylation, each compound was found to be significantly more potent than MTX in inhibiting tumor cell growth in vitro in three lines (L1210, HL60, and S180). The MTX, 5-methyl-5-deazaAMT, and 5-methyl-5-deazaMTX analogues were evaluated in vivo alongside MTX against E0771 mammary adenocarcinoma in mice. All three proved more effective than MTX in retarding the tumor growth. The naphthoyl analogue of 5-deazaAMT strongly inhibited DHFR from *Pneumocystis carinii*, *Toxoplasma gondii*, and rat liver giving IC50 (pM) values of 0.53, 2.1, and 1.6 respectively, but this compound did not inhibit in vitro growth of *T. gondii*, thus indicating lack of transport.

The venerable antitumor agent methotrexate (MTX) owes it cytotoxicity to potent inhibition of dihydrofolate reductase (DHFR; 5,6,7,8-tetrahydrofolate: $NADP^+$ oxidoreductase, EC 1.5.1.3). This enzyme catalyzes reduction of 7,8-dihydrofolate to 5,6,7,8-tetrahydrofolate by NADPH. It can also catalyze reduction of folate to 7,8-dihydrofolate by NADPH, but at slower, species-dependent rates than dihydrofolate to tetrahydrofolate. Without the function of DHFR, cells are deprived of key metabolic intermediates needed to form nucleotides and ultimately nucleic acids.[1-5]

After Prendergast and co-workers cloned the gene that encodes human DHFR and subsequently expressed the enzyme in *Escherichia coli*,[6] Davies and co-workers solved the structure of the human enzyme through high-resolution X-ray crystallographic studies of binary complexes of DHFR with folic acid and 5-deazafolic acid.[7] The coordinates of these structures were filed in the Brookhaven National Laboratories Protein Data Bank.[8] Also in the report by Davies et al., previous reports by others on high-resolution crystallographic studies of DHFR from various sources are reviewed; the binding characteristics of MTX and folate are compared and contrasted, and strong evidence that the presence of NADPH does not alter the orientation of MTX relative to the enzyme is discussed.

Events that led to the investigation described in the present report began with a request from NIH agencies for available compounds qualifying as potential lipophilic antifolates. We supplied a group of reported compounds[9,10] to be tested for inhibitory effects on DHFR from pathogenic organisms and on DHFR from a typical mammalian source. The test results, which we received before publication by Broughton and Queener,[11] showed that two candidates, namely 6-[(1-naphthylamino)methyl]-2,4-diaminopteridine and 6-[(phenylthio)methyl]-2,4-diaminopteridine, exerted greater inhibitory potency against DHFR from *Pneumocystis carinii* (PC) than DHFR from rat liver (RL). The compounds have selectivity ratios (IC_{50} for RL enzyme divided by IC_{50} for PC enzyme) of 9.7 for the naphthylamino and 25.9 for the phenylthio derivative. Although less selective, the naphthylamino compound with IC_{50} vs PC DHFR of 0.13 μM is 73-fold more potent than the phenylthio compound.[11] Prompted by these results, we investigated molecular graphics aspects of the binding of the naphthylamino compound using a model built from the coordinates of *Lactobacillus casei* DHFR[12] obtained from the Protein Data Bank. Especially conspicuous was the large hydrophobic pocket in which the naphthyl group was bound. It appeared that this space could accommodate even larger groups. If extended to DHFR from other sources, this conjecture is supported by the reported inhibitory activity against DHFR from murine and human tumor cells of several nonclassical 2,4-diaminoquinazolines bearing hy-

† Southern Research Institute.
‡ Roswell Park Cancer Institute.
§ Memorial Sloan-Kettering Cancer Center.
® Abstract published in *Advance ACS Abstracts*, November 15, 1993.

0022-2623/93/1836-4161$04.00/0

drophobic side chains consisting of anthracene, phenanthrene, and fluorene groups.[13]

Molecular Modeling. Encouraged by the preliminary graphics observations, with the release by the Protein Data Bank of the recombinant human DHFR coordinates provided by Davies et al.,[7] we began a study to model analogues of classical antifolates such as MTX and aminopterin with the 1,4-disubstituted benzene ring of the side chain replaced by the 1,4-disubstituted naphthalene ring. Our aim was to graphically examine the feasibility of the naphthalene group fitting into the hydrophobic pocket while not disrupting the structural flexibility needed to allow the characteristic hydrogen bonds and electrostatic interactions that allow the extremely tight binding of the parent antifolates to DHFR.

The model structure for our graphics studies was the aminopterin analogue with naphthoyl in place of benzoyl (structure **21b** shown in Scheme II). The modeling effort based on this structure suggests that two energetically accessible binding modes exist for compounds bearing the naphthoyl side chain, differing by an approximately 180° rotation of the aromatic ring about the C1–C4 axis (Figure 1A,B). The calculated energy difference between these two binding modes is approximately 2.7 kcal/mol; however, because of uncertainties inherent to the calculations, because of lack of knowledge concerning the state of solvation of the active site, and because, in the lower energy binding mode (Figure 1A), the naphthalene ring projects beyond what would be the enzyme-solvent interface if the polar medium were adequately modeled, it is impossible to ascertain at this time which of the two modes is preferred. No interconversion between these modes was observed during molecular dynamics runs.

Figure1C depicts the primary hydrophilic contacts in the lowest energy binding mode of the model. The extensive hydrogen-bonded network involving the pteridine ring, the modeled water molecule, and the side chains of W24, E30, and T136, expected from previous analysis,[14] remains intact. There are in addition hydrogen bonds between the 2-NH_2 group and the backbone carbonyl of E30, and between position N-8 and the backbone amide of A9. Although the specific pattern of hydrogen bonding is certainly influenced by the number of water molecules incorporated in the enzyme model, it is clear that even minimal water is sufficient to contribute to the organization of the active site and stabilize ligand binding. Analysis of molecular dynamics trajectories in which the internal cavity was fully solvated indicated that the presence of additional water did not significantly alter binding. In the side chain, the salient polar contacts are the salt bridge between the α-carboxylate and R70, and hydrogen bonds involving both carboxylates and the side chains of Q35 and N64. This latter residue also interacts with the naphthoyl carbonyl oxygen. There is no significant difference in the polar contacts exhibited by the alternative binding geometry, except for the substitution of W24 for A9 in the hydrogen bond to N-8, resulting from a slight rotation of the plane of the heterocyclic system.

The hydrophobic contacts in the enzyme-inhibitor complex are illustrated in Figure 1D. The diaminopteridine ring is parallel to and sandwiched between the phenyl rings of F31 and F34. Although the three rings are somewhat off-center (the centroids do not align), the base-stacking effect is great enough to result in substantial van der Waals contact. The pteridine cavity is lined with hydrophobic residues also contributing to the interaction, including V8, A9, L22, W24, and Y121. The naphthalene ring of the side chain makes van der Waals contacts with L22, I60, and F31 (which is perpendicular to the plane of the naphthalene) and has lesser interactions with L67, V115, and the methyl group of T56. In the alternative, rotated binding mode (Figure 1B), these latter three contacts are enhanced, and a new interaction with F34 is seen, while the influence of L22 to binding is reduced. Significantly, this binding configuration also results in the displacement of the F34 side chain such that a van der Waals contact is made with the isopropyl group of V115, which probably constrains the maximum size of a hydrophobic substituent in this direction. The pocket appears, however, to contain substantial unoccupied volume between the side chains of I60 and L67, projecting back toward M52.

The modeling graphics show that either conformer of the naphthoyl analogue **21b** is entirely compatible with the binding site. Key polar contacts and hydrophobic interactions are seen to be operative. These observations furthered our interest in synthesizing and evaluating naphthoyl analogues as antitumor agents in order to extend structure–activity relationships among classical antifolates. Other questions of interest posed by the naphthoyl analogues are the effects that the larger hydrophobic group would have on the overall antitumor properties, particularly with respect to cell membrane transport and interactions with intracellular loci other than DHFR. In the discussion which follows we describe syntheses of **21b** and analogues and also results from testing of these compounds as antitumor antifolates.

Syntheses. Synthetic work began with development of reaction sequences leading to the naphthoyl-containing side chain precursors which would be coupled with functionalized pteridines and 5-deazapteridines. Two routes to the side chains shown in Scheme Iwere developed. The first route began with commercial 4-amino-1-naphthalenecarbonitrile (**1**), which was hydrolyzed in alcoholic KOH using a reported procedure.[15] The resulting 4-amino-1-naphthoic acid (**2**) was then converted to the known *N*-[(benzyloxy)carbonyl] derivative **3**.[15] Peptide coupling (using diethyl phosphorocyanidate as the carboxyl-activating agent) of blocked intermediate **3** with diethyl L-glutamate afforded N-protected side-chain precursor **4**. Hydrogenolysis of the protective group of **4** then gave diethyl *N*-(4-amino-1-naphthoyl)-L-glutamate (**8**), the precursor to target analogues of aminopterin. The expense of starting material **1** plus the inconvenient stringent hydrolysis step required to convert it to **2** prompted us to seek a more practical route. Such a route was suggested by the reported conversion of 4-nitro-1,8-naphthalic anhydride (**5**) to 4-nitro-1-naphthoic acid (**6**) through a selective decarboxylation process.[16] The ready commercial accessibility of **5** plus the facile conversion of it to **6** made this the route of choice over that beginning with **1**. Coupling of **6** with diethyl L-glutamate gave nitro compound **7**. Our first hydrogenation experiment for conversion of **7** to **8** was carried out in EtOAc containing Raney Ni under H_2 pressure of about 3.4 atm (50 psi); the result was over-hydrogenation giving the tetrahydro derivative **10** instead of the intended **8**. Over-hydrogenation was readily curtailed by carrying out the reaction at atmospheric pressure using H_2 over H_2O in a gas buret and interrupting the process when no more than the calculated

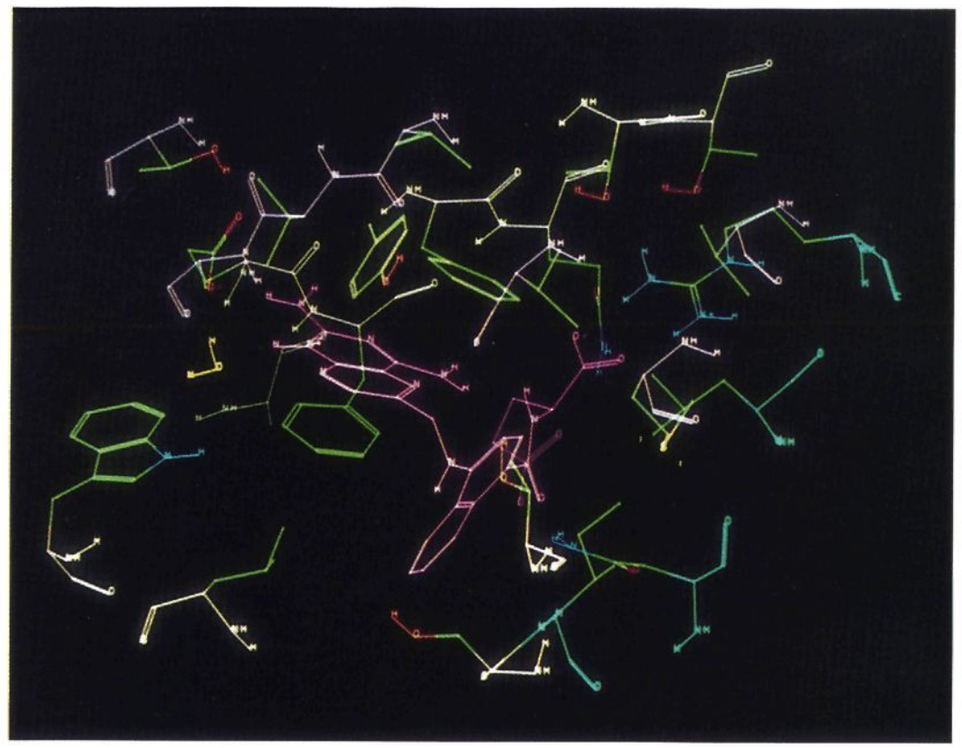

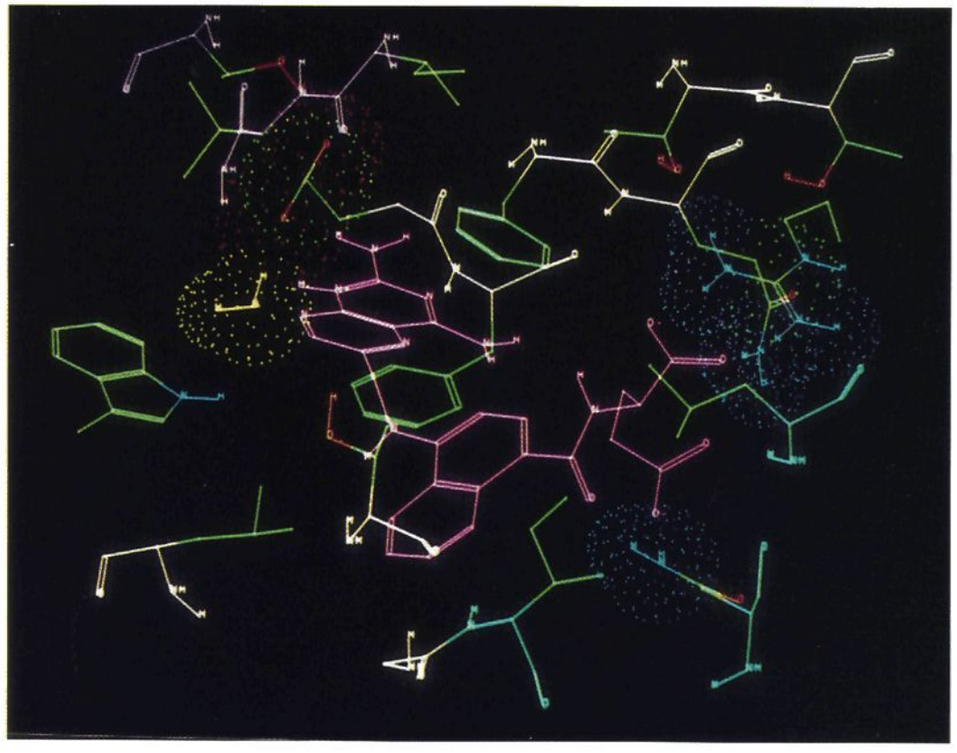

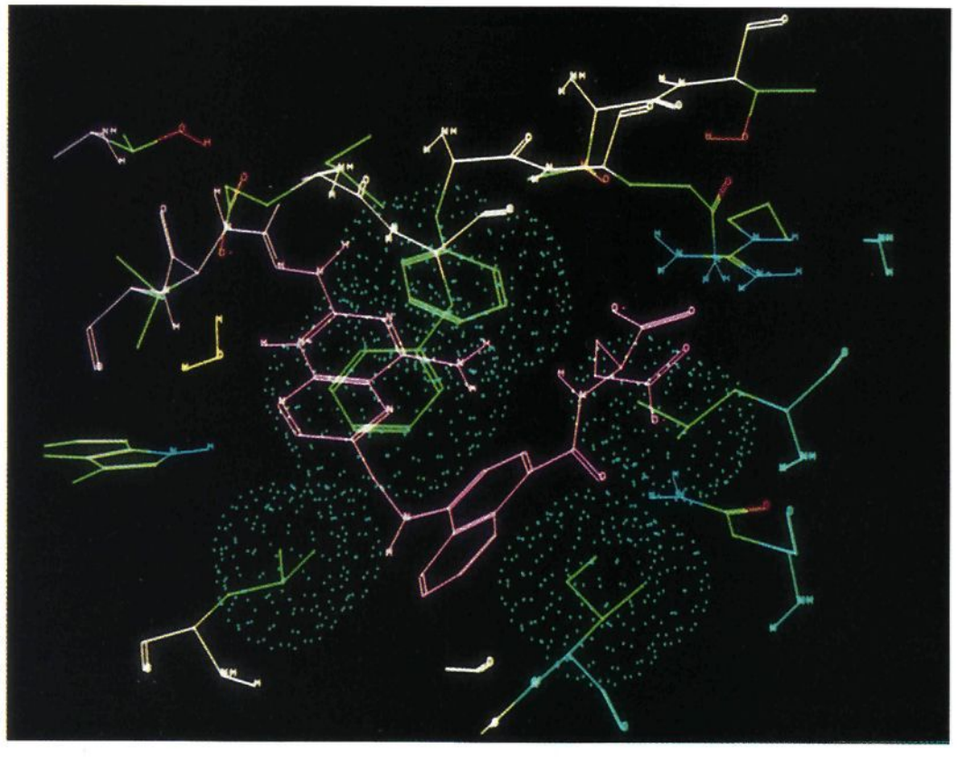

Figure 1. (A, top left; B, top right) The two binding modes of inhibitor within the active-site model. A is the lower energy mode. (C, bottom left) Important polar contacts of enzyme–inhibitor complex. (D, bottom right) Hydrophobic contacts between inhibitor and DHFR. Some active-site atoms have been removed for clarity.

Scheme I. Routes to Side-Chain Precursors 8–10

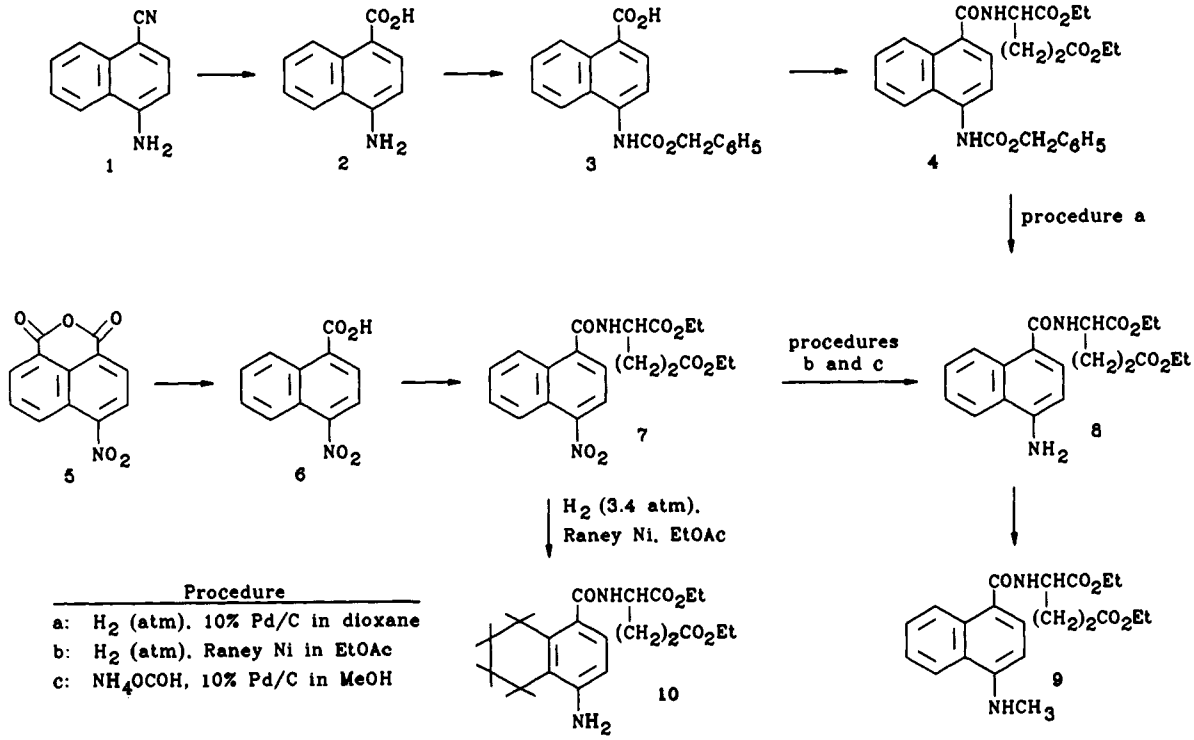

volume of H_2 required to form **8** had been consumed. Pure **8** was obtained after recrystallization. Without interruption of the process at the required H_2 volume, hydrogenation slowly continued with **10** being formed. The best way found to convert **7** to **8** was, however, by a reported general method using ammonium formate with 10% Pd on C in MeOH.[17] This method proved well-suited for this conversion. Reduction of **7** to **8** was complete in 1 h at room temperature. The *N*-methyl derivative **9**, which was needed to prepare the target MTX analogues, was prepared from **8** in two ways: first using an adaptation of a general method in which the *N*-formyl derivative of **8** was reduced by the BH_3–Me_2S complex,[18] then by direct methylation of **8** using dimethyl sulfate. We obtained pure **9** in 44% yield from the BH_3–Me_2S procedure, but purification was tedious. We did not attempt to improve the procedure because pure **9** was more easily obtained in the needed quantity following direct methylation.

Side-chain precursors **8** and **9** were converted to diethyl esters **21a–28a** by one or more of the four general coupling methods designated A–D in Scheme II. Compound types thus prepared include pteridines (**21a**, **22a**), 5-deazapteridines (**23a**, **24a**), 5-methyl-5-deazapteridines (**25a**, **26a**), and a 5,8-dideazapteridine (**27a**). With availability of tetrahydro precursor **10**, we also prepared the side-chain variant **28a**. Methods A, B, and D are known general methods for syntheses of antifolates, but method C has not been used before in this connection. Method A, used in alkylations of **8** and **9** by 6-(bromomethyl)-2,4-diaminopteridine (**11**) to produce **21a** and **22a**, has been a standard method for synthesizing antifolates since **11** was introduced for this purpose in 1974.[19] In method B, we used 5-deaza intermediates bearing the 6-bromomethyl group (structures **17** and **18**,[20–22] Scheme II). Unlike **11**, these compounds are not easily prepared in suitable purity by treatment of their 6-hydroxymethyl precursors (**15** and **16**) with dibromotriphenylphosphorane (Ph_3PBr_2) in Me_2NAc.[20] Both **17** and **18** have, however, been readily prepared by treatment of **15** and **16** with HBr in dioxane.[20,21] In this report, we describe a convenient alternative procedure using HBr in AcOH. Compounds **23a**, **25a**, and **26a** were then prepared using the appropriate bromomethyl intermediates **17** or **18**. Method D, reductive condensation between nitrile and amine, was used in preparations of **23a**, **27a**, and **28a**. The standard procedure[23,24] (in AcOH containing Raney Ni under H_2 at ambient conditions) gave satisfactory results, but its use in preparations of **23a** and **27a** required care to avoid overhydrogenation. The newer approach, method C, with further experimental development work, might have some general future use. The sequence begins with pretreatment of a suspension of hydroxymethyl compound **15** or **16** in Me_2NAc with sufficient Ph_3P and CBr_4 to give a Me_2-NAc-soluble product which we believe is represented by structure **19** or **20** in which the hydroxy group of **15** or **16** has been replaced by Br and the former amino groups have been converted to triphenylphosphinimino groups. The side-chain intermediate **8** or **9** is then added to the reaction solution to undergo alkylation by **19** or **20**; afterward the amino groups are regenerated by treatment of the putative triphenylphosphinimino derivative with glacial AcOH. Compounds **24a**, **25a**, and **26a** were formed in this way. The sequence is based on known analogous reactions of nucleosides with carbon tetrahalides and Ph_3P in Me_2NAc[25–27] and also on the preparation of **11** from its hydroxymethyl precursor by the action of Ph_3PBr_2 (3.3 molar equiv from Ph_3P and Br_2) in Me_2NAc followed by a treatment with glacial AcOH.[19] Further, MTX diethyl ester has been prepared in commercial production scale by a similar sequential process in which the Br compound was formed as in the preparation leading to **11**, then the side chain was introduced for alkylation, and afterward the triphenyphosphinylidene groups were removed by mild HCl hydrolysis.[28] Yields of purified products from methods A–D are listed in Table I. Methods A and B gave the better yields (21–59%) while methods C and D typically produced 15–23% yield.

Diethyl esters **21a–28a** were hydrolyzed to give the target

Scheme II. Intermediates to Naphthoyl Analogues **21b–28b**

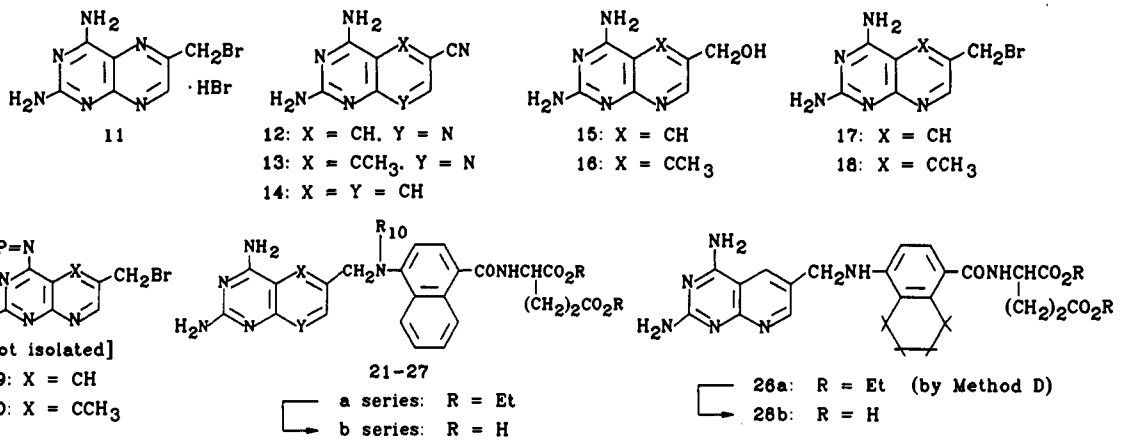

Structure No.	X	Y	R_{10}	Method used in prepn of ester[a]
21	N	N	H	A
22	N	N	CH_3	A
23	CH	N	H	B, D
24	CH	N	CH_3	C
25	CCH_3	N	H	B, C
26	CCH_3	N	CH_3	B, C
27	CH	CH	H	D

[a] Methods of synthesis: A, 6-CH_2Br compound and appropriate side-chain precursor 8 or 9 in Me_2NAc; B, 6-CH_2Br compound 17 or 18 with 8 or 9 in Me_2NAc containing MgO; C, 6-CH_2OH compound 15 or 16 with Ph_3P and CBr_4 in Me_2NAc followed by 8 or 9 and later with AcOH; D, 6-CN precursors 12 or 14 with 8 in reductive condensation.

Table I. Diethyl Esters **21a–28a** Synthesized As Indicated in Scheme II

compd no.	molec formula[a–c]	method	yield, %[d]
21a	$C_{27}H_{30}N_8O_5 \cdot 1.5H_2O$	A	30
22a	$C_{28}H_{32}N_8O_5 \cdot H_2O$	A	59
23a	$C_{28}H_{31}N_7O_5$	B, D	21, 23
24a	$C_{29}H_{33}N_7O_5 \cdot 1.3H_2O$	C	21
25a	$C_{29}H_{33}N_7O_5 \cdot 0.8H_2O$	B, C	36, 17
26a	$C_{30}H_{35}N_7O_5 \cdot 0.65H_2O$	B, C	41, 18
27a	$C_{29}H_{32}N_6O_5$	D	15
28a	$C_{28}H_{35}N_7O_5$	D	15

[a] Anal. C, H, N except for **23a**, **27a**, and **28a** which were not determined. [b] ^1H NMR spectra were obtained on all compounds except **27a** and were consistent with assigned structures. [c] The mass spectrum of each sample was as expected for the assigned structure. [d] After purification by SG chromatography; each sample was homogeneous by TLC.

Table II. Antifolate Analogues **21b–28b** from Hydrolysis of Their Diethyl Esters

compd no.	molec formula[a,b]	yield, %
21b	$C_{23}H_{22}N_8O_5 \cdot 2.5H_2O$	72
22b	$C_{24}H_{24}N_8O_5 \cdot 1.75H_2O$	86
23b	$C_{24}H_{23}N_7O_5 \cdot 2.75H_2O$	62
24b	$C_{25}H_{25}N_7O_5 \cdot 2.0H_2O$	76
25b	$C_{25}H_{25}N_7O_5 \cdot 1.2H_2O$	94
26b	$C_{26}H_{27}N_7O_5 \cdot 1.25H_2O$	90
27b	$C_{25}H_{24}N_6O_5 \cdot 2.2H_2O$	85
28b	$C_{24}H_{27}N_7O_5 \cdot 1.8H_2O$[c]	63

[a] Anal. C, H, N with exception as noted for **28b**. [b] ^1H NMR and mass spectra obtained on each compound were consistent with the assigned structure. [c] Anal. N: calcd 18.64, found 17.96.

compounds **21b–28b** using mild basic conditions. The progress of each of the hydrolytic conversions was followed by HPLC as described in a reported general method.[24] Percentage yields and other data are given in Table II. ^1H NMR spectral data for **21b–27b** are summarized in Table III. Noteworthy highlights among the assigned chemical shifts are the expected distinctions about the C^9–N^{10} bridge regions and the naphthalene 3′-H between aminopterin analogues (**21b, 23b, 25b,** and **27b**) and MTX analogues (**22b, 24b,** and **26b**). Other expected clear differences are between the 5-unsubstituted-5-deaza compounds **23b** and **24b** (doublet near δ 8.3 due to 5-H) and the 5-methyl-5-deaza compounds (singlet near δ 2.75 due to 5-CH_3). Chemical shift values due to remaining parts of the general structure are fairly constant. The 5,8-dideaza analogue **27b** gave the characteristic shifts due to the protons at postions 5, 7, and 8.[23b]

The earlier-mentioned report by Broughton and Queener[11] on selectivity testing was published while the work described in this report was in progress. The samples tested by Broughton and Queener were from an off-the-shelf procurement program, and results from the naphthoyl analogue of MTX (structure **22b** in this report) were included. The origins of tested compounds were not given in the Broughton–Queener report, and the literature does not contain other mention of **22b**.

Biological Studies. Compounds **21b–28b** were evaluated as inhibitors of DHFR from L1210 cells. Their K_i values (see Table IV) show the naphthoyl analogues **21b–27b** to be equal to MTX in inhibitory potency against the isolated enzyme. Only the tetralin analogue **28b** with its greater bulk attendant with the loss of planarity in the annulated ring shows lower potency, that being by a factor of only about 2.7. Surprisingly, transport into L1210 cells measured by influx K_i values (also in Table IV) was enhanced over MTX in each of the compounds. Influx efficiency relative to MTX varied from about 2.5-fold greater for **23b** up to about 6-fold greater for **26b** and **28b**. These results indicating greater affinity by the reduced folate/MTX carrier system for the naphthoyl analogues than for MTX could mean that the carrier protein, like

Table III. Summary of ^{1}H NMR Chemical Shifts for Target Compounds 21b–27b[a]

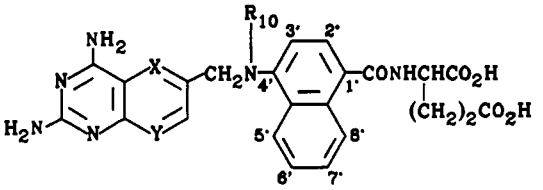

assignments	multiplicity	compound number 21b	22b	23b	24b	25b	26b	27b
CHC*H*$_2$	m	1.89, 2.06	1.90, 2.09	1.90, 2.04	1.92, 2.06	1.91, 2.06	1.91, 2.07	1.88, 2.04
CH$_2$CO	t	2.36	2.39	2.36	2.36	2.36	2.37	2.32
C*H*CH$_2$	m	4.39	4.45	4.40	4.44	4.40	4.4	4.33
CONH	d	8.4	8.68	8.48	8.60	8.3	8.6	8.00
CH$_2$N*H*	t	7.36		7.28		7.3		7.3
C*H*$_2$NH	d	4.68		4.54		4.54		4.54
C*H*$_2$N(CH$_3$)	s		4.51		4.32		4.39	
NCH$_3$	s		2.87		2.78		2.70	
5-CH$_3$	s					2.74	2.77	
5-H	d			8.3	8.28			8.16[b]
7-H	d	8.72	8.70	8.72	8.47	8.51	8.58	7.60
8-H	d							7.23
NH$_2$(2,4-di)	s	6.74, 7.83	6.65, 7.6	6.64, 7.78	6.66, 7.76	7.0, 7.5	6.8, 7.4	7.2–7.5, 8.0
2'-, 6'-, and 7'-H	br m	7.4–7.6	7.4–7.7	7.4–7.6	7.5–7.7	7.4–7.7	7.5–7.6	7.4–7.6
3'-H	d	6.56	7.21	6.46	7.20	6.49	7.35	6.37
5' and 8'-H	m	8.30, 8.38	8.28, 8.42	8.3, 8.4	8.30, 8.39	8.28, 8.40	8.20, 8.30	8.28, 8.42

[a] Spectra determined as described in the Experimental Section. [b] Singlet.

Table IV. In Vitro Comparisons of Naphthoyl Analogues 21b–27b and Tetrahydronaphthoyl Analogue 28b with MTX against L1210, HL60, and S180[a]

compd	L1210 cell DHFR inhibn K_i (pM)	L1210 cell influx K_i (μM)	IC$_{50}$, nM L1210	HL60	S180
MTX	4.82 ± 0.6	3.93 ± 0.4	9.0 ± 1.0	8.1 ± 1.0	10 ± 3.0
21b	4.55 ± 0.5	0.92 ± 0.2	6.0 ± 1.6	4.6 ± 1.0	5.9 ± 2.2
22b	5.22 ± 0.5	1.04 ± 0.3	9.0 ± 1.0	3.3 ± 0.8	9.3 ± 2.0
23b	3.65 ± 0.6	1.52 ± 0.3	4.2 ± 1.0	1.4 ± 0.2	3.9 ± 0.2
24b	4.65 ± 0.6	0.78 ± 0.2	2.3 ± 0.6	1.5 ± 0.3	1.9 ± 0.1
25b	5.08 ± 0.5	1.31 ± 0.2	3.9 ± 0.1	0.74 ± 0.1	3.8 ± 0.1
26b	4.84 ± 0.6	0.66 ± 0.1	2.4 ± 0.4	0.56 ± 0.1	2.6 ± 0.1
27b	5.2 ± 1.0	0.9 ± 0.1	6.1 ± 0.6	0.65 ± 0.03	3.9 ± 0.4
28b	13.1 ± 2	0.6 ± 0.1	16 ± 3	17 ± 1	33 ± 2

[a] Methods described in ref 29.

Table V. Naphthoyl Analogues as Substrates and Inhibitors of CCRF-CEM Folylpolyglutamate Synthetase[a]

compd	K_m, μM	$V_{max,rel}$[b]	V/K	inhibn, %[c]
aminopterin	4.1 ± 1.2	1	0.24	
MTX[d]	42	0.6	0.015	
21b	nd[e]	0.03	nd	12
22b	82 ± 9	0.27 ± 0.01	0.0033	3
23b	nd	0.01	nd	21
24b	nd	0.01	nd	23
25b	nd	0.02	nd	(IC$_{50}$ = 69 μM)
26b	nd	0.04	nd	10
28b	nd	0.01	nd	16

[a] Methods described in the Experimental Section and ref 33. [b] Activity with aminopterin defined as $V_{max,rel}$ = 1. When low activity was detected, $V_{max,rel}$ was defined as the activity measured at 100 μM analogue relative to saturating aminopterin. [c] Inhibition was expressed as the percent inhibition of FPGS activity of 50 μM aminopterin in the presence and absence of 100 μM analogue. For **25b**, the IC$_{50}$ was determined as described in the Experimental Section. [d] Values from ref **33b**. [e] nd = not determined.

DHFR, also has an open space to accommodate bulky groups positioned in the side chain as in these naphthoyl analogues.

The compounds were tested for their ability to inhibit growth in vitro of three tumor cell lines: L1210, HL60, and S180. The IC$_{50}$ values listed in Table IV show each of the compounds except **28b** to be as inhibitory as, mostly more so than, MTX in all three lines. The lower activity of **28b** compared with MTX appears to be commensurate with the 2–3-fold reduction in DHFR inhibitory capacity relative to MTX.

We supplied **23b** (naphthoyl analogue of 5-deazaaminopterin) to be tested for inhibition of DHFR from *P. carinii*, *Toxoplasma gondii*, and rat liver. Results (IC$_{50}$, pM) against DHFR from the source indicated were as follows: *P. carinii*, 0.53; *T. gondii*, 2.1; rat liver, 1.6 (selectivity ratios RL/PC, 3; RL/TG, 0.8).[30] [In the Broughton–Queener report mentioned earlier, **22b** (naphthoyl analogue of MTX) was reported to have IC$_{50}$ vs *P. carinii* DHFR of 0.19 pM and 2.5 pM against rat liver DHFR giving a selectivity ratio of 13.2.[11]] Prompted by the potent inhibitory activity of the naphthoyl analogues against DHFR from these pathogenic organisms, we also supplied **23b** to be tested for ability to inhibit in vitro growth of *T. gondii*. Growth-inhibitory activity would signal cell entry, but **23b** was without effect.[31] This result would indicate, in light of its potent inhibition of isolated *T. gondii* DHFR, that **23b**, like MTX and aminopterin, is not transported into the organism. The added hydrocarbon bulk of **23b** over MTX or aminopterin apparently is not sufficient to permit influx by passive diffusion, and *T. gondii* does not have the active transport system required by classical antifolates for transport through cell membranes.[32]

Studies of naphthoyl analogues **21b–26b** and the tetralin type **28b** as substrates and inhibitors of folylpolyglutamate synthetase (FPGS) from CCRF-CEM cells reveal substrate activity in this series is markedly reduced relative to classical benzoyl analogues (see Table V). Only **22b** (naphthoyl analogue of MTX) showed significant substrate activity, and it was 4.5-fold less active than MTX and over 70 times poorer than aminopterin (compare ratios of V/K listed in Table V). The other analogues tested displayed such weak substrate activity that their K$_m$ values could not be determined. Each of the analogues was only weakly inhibitory to FPGS from CCRF-CEM cells. The extents of polyglutamylation of **21b** and **22b** (naphthoyl

Table VI. Comparisons of Rates of Polyglutamylation of Aminopterin, MTX, 21b, and 22b in L1210 Cells

compd	specific activity of L1210 FPGS, pmol/mg protein per h[a]	compd	specific activity of L1210 FPGS, pmol/mg protein per h[a]
aminopterin	1.91 ± 0.3	MTX	0.38 ± 0.07
21b	0.41 ± 0.09	22b	0.18 ± 0.06

[a] Substrates compared at 100 μM of each; methods described in the Experimental Section and in refs 29 and 33.

Table VII. Antitumor Activity of Naphthoyl Analogues 22b, 25b, and 26b Compared with MTX against the E0771 Mammary Adenocarcinoma[a]

		day 7		day 10		day 14	
compd	dosage[b] (mg/kg)	av tumor[c] (mm^3)	T/C[d] (%)	av tumor[c] (mm^3)	T/C[d] (%)	av tumor[c] (mm^3)	T/C[d] (%)
control		221		624		1732	
MTX	3	180	81	624	100	1437	83
	6	108	49	187	30	540	31
22b	100	82	37	268	43	839	48
	150	62	28	144	23	493	28
25b	3	113	51	421	68	1048	60
	6	87	39	42	7	toxic[e]	
26b	12	108	49	333	53	1048	60
	24	87	39	119	19	493	28

[a] Five mice/test; methods described in ref 29. [b] R_x daily for 5 days starting day 3 after implantation. [c] Vol. (mm^3) = $4/3\pi r^3$. [d] T/C = treated/control. [e] Four toxic deaths.

analogues of aminopterin and MTX, respectively) in L1210 cells were also substantially less than for their classical benzoyl analogues as shown by specific activity data listed in Table VI. The results were conclusive that FPGS from human and L1210 tumor cells has a restriction for catalysis with regard to the bulk that can be tolerated in the side chain of classical antifolates, and, at least in human FPGS, the bulk restriction also applies to binding.

Three representative members of the naphthoyl series were selected for analogy with well-studied classical antifolates[29] and tested in vivo for antitumor activity. The MTX analogue **22b** and both 5-methyl-5-deazapteridine types **25b** and **26b** were tested alongside MTX in mice against the E0771 mammary adenocarcinoma. Results are listed in Table VII. A surprising spread in toxicity toward mice was observed. The maximum tolerated dose of **25b** was the same as that of MTX (6 mg/kg), and that of **26b** was 4-fold greater, but that of **22b** was 25-fold greater (150 mg/kg). Although **25b** proved to be toxic at the day-14 observation of tumor volume, each of the three compounds proved to be more effective than MTX in reducing the solid tumor volume. Comparing the influx and FPGS data with the in vivo results for the three compounds does not account for the markedly lower toxicity of **22b**. In fact, only **22b** had measurable substrate activity with FPGS. The relatively facile influx of these potent DHFR inhibitors would be expected to produce a compensating effect for poor intracellular polyglutamylation, but the differences in toxicity toward mice are unaccountable from the available data.

These studies show that computer-generated molecular graphics derived from X-ray crystallography data can aid in the design of inhibitors of DHFR, but drug design considerations regarding cell membrane transport and intracellular polyglutamylation must rely for the present on structure–activity relationships.

Experimental Section

Molecular Modeling. All calculations were performed on a DEC VAX 6420 computer system under VMS 5.4, connected to an Evans and Sutherland PS390 graphics station, using the MACROMODEL Version 3.0[34] and SYBYL Version 5.41[35] software packages. Molecular dynamics was conducted under MACROMODEL Version 3.5 on a Silicon Graphics, Inc., IRIS 4D/35TG+. Coordinates for the human DHFR binary complex with folate[7] were obtained from the Brookhaven Protein Databank[8] (structure code 1DHF). Of the two molecules in the asymmetric unit, molecule two (terminology of Davies et al.[7]) was chosen for model construction since it was the more ordered; however, the two structures are largely similar except for packing environment. After conversion of coordinates to the appropriate formats, waters of crystallization were deleted from the model with the exception of water molecule 401, which was retained in the active site hydrogen-bonded to folate O4, the indolic nitrogen of W24, and the γ-carboxylate of E30. Hydrogen atoms were added to the structure in their idealized positions. During refinement, the AMBER all-atom molecular mechanics force field[36] as implemented in MACROMODEL was used throughout, employing the Polak–Ribiere conjugate gradient minimization algorithm with extended nonbonded cutoffs (8 Å vdw, 20 Å electrostatic) and constant dielectric constant (1.0). A continuum solvation model[37] was employed during refinement of isolated substrates/inhibitors, whereas solvation was not modeled for bound enzyme complexes.

Initially, only the folate was refined, with protein residues within 5 Å of the ligand incorporated in shells with distance-dependent restraining forces; partial residues on the periphery were incorporated in their entirety. As refinement progressed, additional residues were added to the freely-minimizing substructure, so that ultimately the model consisted of an ellipsoidal volume approximately 20 × 20 × 16 Å centered on the ligand. In addition to the inhibitor and water molecule 401, the following residues composed the freely-minimizing active-site substructure for all subsequent computations: I7, V8, A9, L22, W24, R28, E30, F31, F34, Q35, T38, T39, V50, M52, T56, S59, I60, N64, L67, R70, V115, Y121, T136. As before, residues within 5 Å of this substructure were incorporated with distance-dependent anchoring constants.

The robustness of the model can be judged by comparing the AMBER-minimized folate complex with the corresponding X-ray structure. Qualitatively, the two active sites were identical, despite the deletion of significant numbers of water molecules. There was only a 0.215-Å rms deviation in heavy atom positions between the calculated and observed folate ligands; this variation was primarily a result of a rotation of approximately 15° of the plane of the side chain benzoyl moiety. Not surprisingly, since the γ-carboxyl terminus of the ligand is fully solvent-exposed, deletion of water perturbed several atomic positions in this region, though these shifts had no effect on the remainder of the structure. Thus, the glutamate γ-methylene and γ-carboxylate carbon atoms were displaced 0.326 and 0.290 Å, respectively, from their X-ray coordinates, and there was a slight lengthening of the salt bridge between the folate α-carboxylate and R70 (rms deviation of the O···N distances, 0.443 Å). The salt bridge between the pteridine ring and E30 was unaffected by modeling (rms deviation, 0.056 Å).

Using the MULTIC submode of MACROMODEL, inhibitors were subjected to an internal coordinate tree-search,[38] followed by partial minimization of the resulting conformer sets using BATCHMIN version 3.1.[39] Promising structures were then fully minimized with aqueous solvation (gradient rms ≤ 0.01 kcal/Å-mol), and the resulting lowest energy conformation, presumed to represent the global minimum, was used later for estimation of relative binding enthalpy. All inhibitors based on the 2,4-diaminopteridine ring system were modelled in the N-1 protonated form.[14] Inhibitor structures were then interactively docked to the DHFR active site model, unfavorable contacts were removed using the simplex translation/rotation search feature of MACROMODEL ORIENT submode, and the resultant complex subjected to several cycles of interactive minimization prior to full minimization using BATCHMIN. Finally, Monte Carlo techniques[38] were employed to search for the optimum

binding geometry of the enzyme ligand model. Specifically, the MCMM global search algorithm of BATCHMIN was used with 2–9 randomly selected degrees of freedom varied at each MC step, involving translations and/or rotations of the inhibitor and active site water molecules, as well as torsions of all inhibitor nonring bonds. The model is currently being refined to include active-site side chain torsions in the MC search, with a larger number of torsions varied at each step. To ensure that favorable binding modes would not be missed, a wide energy window was employed (50 kcal) with 500 molecular mechanics iterations executed for each trial structure. During the latter stages of the search, the number of refinement iterations was reduced to 300–350. Monte Carlo simulations were begun from several potential binding modes to reduce the local minimum problem,[40] and the search was continued until no new, significantly different low energy binding conformations were observed. The lowest energy geometries were subsequently fully minimized. For comparative purposes, the modeling program was also carried out on methotrexate and trimethoprim.

For the dynamics simulations, a variable number of explicit water molecules were randomly distributed throughout the binding site. After minimization using expanded cutoffs (12 Å vdw, 25 Å electrostatic) and the continuum solvation model,[37] constant temperature dynamics (either 350 °C or 400 °C) was carried out for 5 ps of equilibration (time step 0.5 fs), followed by 10–15 ps of data sampling (time step 1.0 fs).

Synthetic Procedures. Examinations by TLC were performed on Analtech precoated (250-μm) silica gel G(F) plates. Column chromatographic purifications were done with silica gel (Merck, 60 A, 230–400 mesh for flash chromatography). When solubility limitations made it necessary, crude products to be purified were dispersed in silica gel for application to the column. Dispersal was achieved by evaporating in vacuo a solution of the crude product in DMF containing suspended silica gel (3 g of 60–200 mesh per g of crude product). Evaporations were performed with a rotary evaporator; higher boiling solvents (DMF, Me_2NAc) were removed in vacuo (<1 mm, bath to 35 °C) and more volatile solvents with a H_2O aspirator. Products were dried in vacuo (<1 mm) at 22–25 °C over P_2O_5 and NaOH pellets. Final products were dried and then allowed to equilibrate with ambient conditions of the laboratory. Analytical results indicated by element symbols were within ±0.4% of the theoretical values. Spectral determinations and elemental analyses were performed in the Molecular Spectroscopy Section of Southern Research Institute under the direction of Dr. W. C. Coburn, Jr. The ^1H NMR spectral data reported were determined in Me_2SO-d_6 with a Nicolet NMC 300 NB spectrometer using Me_4Si as internal reference. Chemical shifts (δ) listed for multiplets were measured from the approximate centers, and relative integrals of peak areas agreed with those expected for the assigned structures. Mass spectra were recorded on a Varian MAT 311A mass spectrometer in the fast-atom-bombardment (FAB) mode. UV spectra were determined with a Perkin-Elmer Model Lambda 9 spectrometer. Samples were first dissolved in EtOH, and the solutions were then diluted 10-fold with the medium given in the listings. Maxima are expressed in nanometers with the molar absorbance given in parentheses. Molecular weights used in all calculations conform with the compositions listed with the indicated elemental analyses.

4-Nitro-1-naphthoic acid (6) was prepared from commercially available 4-nitro-1,8-naphthalic anhydride (5) by a reported procedure.[16] The crude product was recrystallized from glacial AcOH, then from EtOH–H_2O: yield 64% (28.7 g from 50 g of 5); mp 219–221 °C (lit.[16] mp 225–226 °C). Further recrystallization from glacial AcOH did not change the melting point.

Diethyl *N*-(4-Nitro-1-naphthoyl)-L-glutamate (7). A solution of diethyl phosphorocyanidate (28.9 g, 0.177 mol) in DMF (170 mL) was added to a stirred solution of 6 (38.4 g, 0.177 mol) and diethyl L-glutamate hydrochloride (42.5 g, 0.177 mol) in DMF (715 mL) at 0–5 °C (bath temperature) followed immediately by a solution of Et_3N (35.7 g, 0.353 mmol) in DMF (170 mL). The reaction solution was left at 20–23 °C for 5 days before most of the DMF was removed in vacuo. The residue was stirred with $CHCl_3$ (1.8 L) and H_2O (0.5 L), then the $CHCl_3$ layer was washed sequentially with 0.5-L portions of H_2O, 0.1 N HCl, H_2O, and saturated NaCl solution before it was dried ($MgSO_4$) and evaporated to give crude 7 as a yellow oil. Pure 7 crystallized from a clarified EtOH solution (0.5 L) of the oil upon gradual addition of H_2O: yield 78% (55.6 g); mp 84–85 °C; MS *m/e* 403, MH^+; homogeneous by TLC (EtOAc-cyclohexane, 1:1). Anal. ($C_{20}H_{22}N_2O_7$) C, H, N.

Diethyl *N*-[4-[[(Benzyloxy)carbonyl]amino]-1-naphthoyl]-L-glutamate (4). This compound was prepared from 4-[[(benzyloxy)carbonyl]amino]-1-naphthoic acid[15] (3) in the manner described above for the analogous nitro compound 7 except that *N*-methylmorpholine was used in place of Et_3N: yield 63% (4.27 g from 4.10 g, 12.8 mmol of 3); mp 117–119 °C (white needles from EtOH–H_2O); MS *m/e* 507, MH^+; homogeneous by TLC (EtOAc-cyclohexane, 1:1). Anal. ($C_{28}H_{30}N_2O_7$) C, H, N.

Diethyl *N*-(4-Amino-1-naphthoyl)-L-glutamate (8). Samples of 8 prepared by the three procedures that follow (routes shown in Scheme I) proved identical with respect to melting point, mixture melting point, IR and mass spectra, and TLC ($CHCl_3$–MeOH, 99:1, and EtOAc–cyclohexane, 1:1). **Procedure a: Hydrogenolysis of 4.** A solution of 4 (2.98 g, 5.88 mmol) in dioxane (55 mL) containing 10% Pd/C (0.55 g) at ambient conditions was stirred under H_2 (over H_2O in a gas buret) until absorption ceased (153 mL). The filtered solution was evaporated, and the residue was recrystallized from EtOAc–cyclohexane to give 8, mp 104–106 °C, in 88% yield (1.93 g). Spectral data: ^1H NMR δ 1.15–1.25 (2 t overlapping, CH_3), 1.96, 2.10 (2 m, $CHCH_2$, nonequivalent), 2.48 (t, CH_2CO), 4.02–4.18 (2 q overlapping, CH_2CH_3), 4.45 (m, NHC*H*), 6.18 (s, NH_2), 6.64 (d, C^3-H), 7.35–7.46 (br m, C^6-H and C^7-H overlapping), 7.48 (d, C^2-H), 8.12 (d, C^5-H), 8.37 (d, C^8H), 8.46 (d, CONH); UV λ_{max} 283 (ϵ 6990) at pH 1, 328 (ϵ 9700) at pH 7, 327 (ϵ 9270) at pH 13. Anal. ($C_{20}H_{24}N_2O_5$) C, H, N. **Procedure b: Raney Ni-Promoted Reduction of 7.** Hydrogenation of 7 (1.00 g, 2.49 mmol) in EtOAc (15 mL) containing Raney Ni (approximately 1 g) was carried out at ambient conditions until 165 mL of H_2 had been taken up (from a gas buret as above). This required about 2.5 h. The filtered solution was concentrated to 10 mL. Addition of cyclohexane (15 mL) caused precipitation of crystalline 8: yield 92% (0.85 g); mp 104–105 °C. In a scaled-up run (using 19.0 g, 47.2 mmol, of 7), the filtered EtOAc solution was evaporated to dryness, and the residue was recrystallized from the minimum of EtOH (about 50 mL) to give 8 in 81% yield (14.2 g). **Procedure c: Reduction of 7 by Ammonium Formate in MeOH Promoted by Pd on C.** A solution of 7 (402 mg, 1.00 mmol) and ammonium formate (290 mg, 4.60 mmol) in MeOH (3 mL) was stirred under N_2 with 10% Pd/C (60 mg). After 1.25 h, TLC ($CHCl_3$-MeOH, 99.1) showed complete conversion. Evaporation of the filtered solution gave an oily residue which was distributed between $CHCl_3$ and H_2O (5 mL of each). Evaporation of the H_2O-washed and dried (Na_2SO_4) $CHCl_3$ layer gave an oil which crystallized readily from EtOAc (5 mL) upon dilution with cyclohexane (35 mL): yield 78% (289 mg); mp 105–107 °C. Anal. ($C_{20}H_{24}N_2O_5$) C, H, N. In a scaled-up run, a solution of 7 (18.0 g, 44.7 mmol) and ammonium formate (13.0 g, 0.206 mol) in MeOH (160 mL) was treated under N_2 with 10% Pd/C (2.7 g). The mixture was stirred under N_2 with moderate external cooling to maintain the temperature below 30 °C. After 1 h, TLC showed only the sought 8. [Approximate R_f values in cyclohexane–EtOAc (1:1) and $CHCl_3$–MeOH (99:1), respectively: for 7, 0.67 and 0.55; for 8, 0.35 and 0.22]. Evaporation of the filtered solution gave a solid residue which was stirred with cold H_2O and collected: yield 92% (15.3 g); mp 104–107 °C, homogeneous by TLC. The pale-yellow product was precipitated from EtOAc solution by addition of cyclohexane to give white crystalline 8, mp 106–107 °C, in 82% yield (13.7 g).

Diethyl *N*-(4-Amino-5,6,7,8-tetrahydro-1-naphthoyl)-L-glutamate (10). Hydrogenation of 7 (2.90 g, 7.21 mmol) in EtOH (150 mL) containing Raney Ni (about 4 g damp) was carried out at 3.1–3.4 atm (about 45–50 psi) overnight in a Parr shaker. TLC (cyclohexane–EtOAc, 1:1) revealed only one spot, but evaporation of the filtered solution gave a residue (2.47 g) whose mass spectrum showed peaks of *m/e* 373 and 377, which are the MH+ values for 8 and a tetrahydro derivative. This residue was recrystallized from EtOAc by addition of cyclohexane. The recrystallized material (1.9 g) still appeared by TLC to be identical with 8, but it had a melting point higher than that of 8 (116–118 °C vs 104–106 °C), and its mass spectrum showed it to be mainly a tetrahydro

derivative. This sample and the residue from evaporation of the mother liquor from its recrystallization were combined in EtOH (100 mL) along with Raney Ni as originally, and the mixture was again treated with H_2 under 3.4 atm of pressure (50 psi) on a Parr apparatus for about 18 h. Removal of the catalyst and evaporation afforded only the tetrahydro derivative as evidenced by its mass spectrum, *m/e* 377, MH^+. A sample for analysis was reprecipitated from EtOAc by addition of cyclohexane. ^1H NMR spectral data given below established the product to be the 5,6,7,8-tetrahydro derivative **10**, mp 123–125 °C. Anal. ($C_{20}H_{28}N_2O_5$) C, H, N. Spectral data: ^1H NMR δ 1.10–1.25 (2 t overlapping, CH_3), 1.60 (m, C^6H_2 or C^7H_2), 1.72 (m, C^7H_2 or C^6H_2), 1.90, 2.03 (2 m, $CHCH_2$, nonequivalent), 2.30–2.48 (overlapping m due to CH_2CO and C^5H_2 or C^8H_2), 2.72 (t, C^8H_2 or C^5H_2), 4.00–4.16 (2 q, overlapping, CH_2CH_3), 4.32 (m, NHC*H*), 5.06 (s, NH2), 6.44 (d, C^3-H), 6.96 (d, C^2-H), 8.14 (d, CONH); UV λmax 272 nm (ϵ 820) at pH 1, 264 nm (ϵ 9450) at pH 7, 261 nm (ϵ 9340) at pH 13.

Diethyl *N*-[4-(Methylamino)-1-naphthoyl]-L-glutamate (9). Preferred Procedure. Direct Methylation of 8. A solution of **8** (13.6 g, 36.5 mmol), (*i*-Pr)$_2$NEt (5.65 g, 43.7 mmol), and Me_2SO_4 (5.33 g, 42.3 mmol) in DMF (90 mL) was kept near 65 °C (bath temperature) for 21 h. More Me_2SO_4 (1.33 g) was added, and heating as before was continued 4 h longer. The solution was evaporated in vacuo, and the oily residue (29.9 g) was dissolved in EtOH–cyclohexane (60 mL of 1:1). This solution was applied to a column of silica gel (10 × 60 cm of 230–400 mesh poured from cyclohexane). The column was first eluted with cyclohexane (4 L) and then with cyclohexane–EtOAc (3:2). Examination by TLC of fractions from the latter eluant revealed intermediate fractions homogeneous in **9**. The homogeneous fractions were both preceded and followed by bordering fractions with **9** in dominance but containing slight contaminants. Remaining material on the column was eluted with cyclohexane–EtOAc (1:1) to give only unchanged **8**. The yield of pure **9**, mp 106–108 °C, was 27% (3.77 g); mass spectrum, *m/e* 387, MH^+. Anal. ($C_{21}H_{28}N_2O_5$) C, H, N. (Combined fractions that bordered those homogeneous in **9** contained 0.7 g.) The recovery of unchanged **8**, mp 105–106 , was 24% (3.3 g); mass spectrum, *m/e* 373, MH^+. **Alternative Procedure. Methylation of 8 via Formylation followed by BH_3–Me_2S Reduction.**[18] Formylation of **8** (1.65 g, 5.00 mmol) was carried out by the general procedure.[18] The *N*-formyl derivative, obtained as a white solidified foam (homogeneous by TLC, cyclohexane–EtOAc, 1:1; MS *m/e* 401, MH^+ for $C_{21}H_{24}N_2O_6$), was treated with BH_3–Me_2S (12.5 mmol) as described in the reported general procedure. After that point, the procedure was modified. After 15 min at 0 °C, the solution was allowed to warm and was kept 0.5 h at 20–23 °C instead of 2 h at 65 °C as in the reported general procedure. (This change was based on TLC observations made while monitoring the reduction and on results from a trial run in which the higher temperature caused formation of unwanted coproducts.) The solution was then chilled to 0 °C and treated with dry HCl–saturated EtOH (4.7 mL). Stirring under N_2 at 0 °C for 1 h was followed by evaporation to dryness. The residue was stirred vigorously with a mixture of EtOAc and H_2O (125 mL of each) while the mixture was treated with sufficient 1 N NaOH to bring the pH of the aqueous phase to between 8 and 9. The EtOAc layer was washed with H_2O, dried (Na_2SO_4), filtered, and evaporated. Purification on a silica gel column afforded 560 mg of pure **9**; additional pure product (293 mg) was obtained when bordering fractions from the column were purified further by preparative TLC. Pure **9** thus obtained in 44% yield was identical with the analytically pure material obtained after direct methylation of **8** described above.

6-(Bromomethyl)-2,4-diaminopyrido[2,3-*d*]pyrimidine (17) was prepared from 2,4-diaminopyrido[2,3-*d*]pyrimidine-6-methanol[20] (**15**) as described below for the 5-methyl compound **18**. Results were similar, and this intermediate was assigned the formulation $C_8H_8BrN_5 \cdot 1.7HBr \cdot 0.25CH_3CO_2H$. Spectral data: MS *m/e* 254 and 256, MH^+; ^1H NMR (Me_2SO-d_6) δ 4.92 (s, CH_2), 8.84 (d, C^5-H), 8.87 (d, C^7-H).

6-(Bromomethyl)-2,4-diamino-5-methylpyrido[2,3-*d*]pyrimidine (18). 2,4-Diamino-5-methylpyrido[2,3-*d*]pyrimidine-6-methanol[20] (**16**) (4.5 g, 22.0 mmol) was dissolved in glacial AcOH (200 mL) at 95 °C. The solution was cooled to 25 °C, and then treated with stirring with 30% dry HBr in AcOH (400 mL). When addition was complete, a clear solution remained. The flask was stoppered, and the solution was kept at 20–25 °C for 48 h before it was added to Et_2O (2.2 L) with stirring. The precipitate that formed was collected under N_2, washed with Et_2O, and dried; yield 9.5 g of 18 hydrobromide solvated by AcOH; yield 99% (based on formulation shown below). Spectral data: MS *m/e* 268 and 270, MH^+ for $C_9H_{10}BrN_5$; ^1H NMR δ 2.78 (s, 3, CH_3), 4.93 (s, 2, CH_2Br), 8.17 (s, 2, NH_2), 8.75 (s, 1, C_7H), 9.32 (s, 2, NH_2); solvation by CH_3CO_2H evidenced by CH_3 singlet at δ1.90 whose integral height is half that due to the CH_3 of **18**. Thus the molar ratio of **18** to CH_3CO_2H is 1:0.5. Anal. ($C_9H_{10}BrN_5 \cdot 1.7HBr \cdot 0.5CH_3CO_2H$) C, H, N.

Preparations of Esters 21a–27a. The esters were prepared by one or more of the four methods A–D as indicated in Scheme II. Results are listed in Table I. A procedure illustrating each method follows. **Method A. Diethyl *N*-[4-[[(2,4-Diamino-6-pteridinyl)methyl]methylamino]-1-naphthoyl]-L-glutamate (22a).** A mixture of **11**[19,22] (365 mg of 85% purity, 0.923 mmol) and **9** (386 mg, 1.00 mmol) with Me_2NAc (5 mL) was stirred at 20–23 °C under N_2 in a stoppered flask wrapped in Al foil for 5 days. The resulting orange solution was added to stirred H_2O (40 mL) containing Na_2CO_3 (110 mg) to give a yellow solid. The dried solid (510 mg) was dissolved in EtOH (40 mL) for dispersal in silica gel. Evaporation followed, and the dispersion was pulverized and then applied to a silica gel column (200 mL) poured from $CHCl_3$–MeOH–concentrated NH_4OH (90:10:0.5). Elution with the same solvent followed, and fractions 5–15 of approximately 7 mL each were homogeneous (TLC) in product. These fractions were combined and evaporated. The yellow residue was collected with the aid of Et_2O to give pure **22a** (313 mg). Additional data is given in Table I.

Method B. Diethyl *N*-[4-[[(2,4-Diamino-5-methylpyrido-[2,3-*d*]pyrimidin-6-yl)methyl]methylamino]-1-naphthoyl]-L-glutamate (26a). A mixture of 18·1.7HBr·0.5AcOH (500 mg, 1.1 mmol), MgO (44 mg, 1.1 mmol), and **9** (425 mg, 1.1 mmol) in Me_2NAc (8 mL) was stirred at 20–23 °C for 4–5 days. The mixture was filtered (Celite mat), and the filtrate was stirred with silica gel (3.0 g of 60–200 mesh) and then evaporated in vacuo. The residue was pulverized and placed on a silica gel column (as in method A above) poured from $CHCl_3$–MeOH–concentrated NH_4OH (70:10:0.4). Elution with the same solvent gave fractions (numbers 9–13 of 15 mL each) homogeneous in **26a**. Evaporation of the pooled fractions gave pure product (264 mg).

Method C. Diethyl *N*-[4-[[(2,4-Diaminopyrido[2,3-*d*]pyrimidin-6-yl)methyl]methylamino]naphthoyl]-L-glutamate (24a). A solution of **16** (191 mg, 1.00 mmol), Ph_3P (787 mg, 3.00 mmol), and CBr_4 (995 mg, 3.00 mmol) in Me_2NAc (10 mL) was kept at 20–23 °C for 24 h and then treated with **9** (386 mg, 1.00 mmol). The solution was left at 20–23 °C under N_2 in a stoppered flask for 5 days. Solvent was removed in vacuo. and the residue was dissolved in glacial AcOH (2 mL). This solution was heated at 80 °C (bath temperature) for 6–8 min before the AcOH was removed in vacuo. The gummy residue was dissolved in $PhCH_3$ (10 mL), and this solution was treated with Et_2O to precipitate crude product. The Et_2O–$PhCH_3$ supernatant was decanted, and the process of precipitating the crude from $PhCH_3$ by addition of Et_2O was repeated. Mass spectral examination of the crude product mixture showed the expected major peak of *m/e* 560 (MH^+ for the sought **24a**) plus lesser peaks of *m/e* 820 (MH^+ for $C_{47}H_{46}N_7O_5P$, the mono(triphenylphosphinylidene) derivative of **24a**), 387 (MH^+ for starting **9**), 355 (MH^+ for $Ph_3P{=}CHBr$), and 279 (MH^+ for Ph_3PO). This material was dispersed in silica gel in DMF, and after evaporation, the pulverized dispersion was applied to a silica gel column (30 × 4-cm), poured from $CHCl_3$–MeOH–concentrated NH_4OH (95:5:0.1). Initial elution by the same solvent system was followed by a change in $CHCl_3$–MeOH ratio to 9:1 and then to 4:1 after about 400 mL of eluate had been collected. Fractions 1–5 of about 20 mL each eluted by $CHCl_3$–MeOH (4:1) appeared by TLC to be nearly homogeneous in **24a**, but the residue from evaporation of the pooled fractions produced a mass spectrum that revealed continued presence of the peak of *m/e* 820 corresponding to the triphenylphosphinylidene derivative of **24a**. A treatment with glacial AcOH (1 mL) at 80 °C for 4 min followed by evaporation of AcOH and repeated

reprecipitations from $PhCH_3$–Et_2O as described earlier finally gave pure **24a** (125 mg).

Method D. Diethyl *N*-[4-[[(2,4-Diamino-6-quinazolinyl)methyl]amino]-1-naphthoyl]-L-glutamate (27a). A mixture of 14[23a] (130 mg, 0.70 mmol), 8 (261 mg, 0.70 mmol), and Raney Ni (0.3 g of 50% slurry with H_2O) in glacial AcOH (10 mL) was stirred at ambient conditions under H_2 (which was over H_2O in a gas buret) for 3 h (or until H_2 absorption had ceased at 32 mL). The catalyst was removed, and the filtrate was evaporated to near dryness. The residue was dissolved in EtOH, and the solution was added dropwise to stirred 3% Na_2CO_3 solution. The precipitated product was collected, dried, and then dissolved in the minimum of $CHCl_3$–MeOH (7:1) for application to a short column of silica gel. Combined fractions eluted by $CHCl_3$–MeOH (7:1) and homogeneous in expected product according to TLC (3:1 $CHCl_3$–MeOH, R_f ~0.5) were evaporated to give pure **27a** as a light beige solid (56 mg).

Diethyl *N*-[4-[[(2,4-Diaminopyrido[2,3-*d*]pyrimidin-6-yl)methyl]amino]-5,6,7,8-tetrahydro-1-naphthoyl]-L-glutamate (28a) was prepared by reductive condensation of 12 with tetrahydro precursor 10 as above (under method D) for preparation of **27a**; workup and results were similar to those for **27a**. The pure product gave spectra supportive of the assigned structure. Spectral data: MS *m/e* 550, MH^+ for $C_{28}H_{35}N_7O_5$; ^1H NMR δ 1.10–1.20 (2 t overlapping, CH_3), 1.63 (m, C^6H_2 or C^7H_2), 1.78 (m, C^7H_2 or C^6H_2), 1.90, 2.00 (2 m, $CHCH_2$ nonequivalent), 2.38 (t, CH_2CO), 2.50 (m, (C^5H_2 or C^8H_2), 2.73 (t, C^8H_2 or C^5H_2), 4.00–4.15 (2 q overlapping, CH_2CH_3), 4.30 (m, NHCH), 4.40 (d, CH_2NH), 5.85 (t, CH_2NH), 6.28 (d, C^3-H), 6.69 (s, NH_2), 6.98 (d, $C^{2'}$-H), 7.86 (s, NH_2), 8.15 (d, CONH), 8.42 (narrow d, C^5-H), 8.64 (narrow d, C^7-H).

Preparation of Acids 21b–28b by Hydrolysis of the Corresponding Esters. The conversion of **25a** to **25b** described below is illustrative of the mild saponification procedure used for each of the conversions. Results are listed in Tables II and III. ***N*-[4-[[(2,4-Diamino-5-methylpyrido[2,3-*d*]pyrimidin-6-yl)methyl]amino]naphthoyl]-L-glutamic Acid (25b).** A solution of **25a** (250 mg, 0.436 mol) in MeOH (45 mL) containing 1 N NaOH (0.96 mL) was kept at 20–25 °C under N_2 for 3 days in a stoppered flask wrapped in Al foil. MeOH was removed by evaporation, and the residue was dissolved in H_2O (15 mL) to which 1 N NaOH (0.48 mL) had been added. After this solution had been kept 24 h longer, HPLC showed the conversion to be complete. The solution was then treated with stirring with 1 N HCl to pH 3.8, and after a refrigeration period, the precipitated pale-yellow solid was collected, washed with cold H_2O, and dried: yield 94% (215 mg); homogeneous (>99%) by HPLC.[24] Additional data is given in Tables II and III.

Effects on Human Folylpolyglutamate Synthetase (FPGS). Results obtained as described below are listed in Table V.

Radiolabeled Reagents. L-[2,3-^{3}H]Glutamic acid (20 Ci/mmol) was obtained from New England Nuclear (Boston, MA).

Enzyme Assays. FPGS was assayed[33a,b] using L-[^{3}H]Glu as a substrate and DEAE-cellulose minicolumns to separate free L-[^{3}H]Glu from that ligated to a folate substrate. Standard assay mixtures (0.25 mL, pH 8.4 at 37 °C) containing 100 mM Tris-HCl, 5 mM ATP, 10 mM $MgCl_2$, 20 mM KCl, 100 mM 2-mercaptoethanol, 4 mM L-[^{3}H]Glu (≈2 cpm/pmol), 50 μM aminopterin, and enzyme were incubated at 37 °C. One unit of FPGS activity is defined as the incorporation of 1 pmol of L-[^{3}H]-Glu/h under standard conditions. Aminopterin was replaced by analogues as indicated; analogues were tested for substrate activity over the range 0–100 μM, except for **22b** where 0–200 μM was used to obtain an accurate K_m value. It was verified that each parent compound eluted from assay columns during the acid wash that is used to elute polyglutamate products; thus, although polyglutamate standards of each compound were not available, any polyglutamate products formed should also have eluted in this fraction and been quantifiable. Enzyme assays were performed in duplicate or triplicate under conditions of enzyme and time linearity, and each complete experiment was repeated at least once. Kinetic data were analyzed by standard means.[33] Inhibitory potency was initially determined by comparing the activity of 50 μM aminopterin in the presence and absence of 100 μM analogue. If inhibition exceeded 50%, the concentration of drug inhibiting FPGS activity by 50% (IC_{50}) was determined under standard conditions with 50 μM aminopterin as substrate.

Enzymes. FPGS from CCRF-CEM cells was prepared by fractionating freeze–thawed lysates (in 100 mM Tris-HCl, pH 8.85 containing 100 mM 2-mercaptoethanol, 2.5 mM benzamidine, and 0.1 mM EDTA) with $(NH_4)_2SO_4$ (0–40% saturation pellet) followed by gel sieving chromatography (BioGel A-0.5M). Active fractions (in 20 mM potassium phosphate, pH 7.5 containing 500 mM KCl, 50 mM 2-mercaptoethanol, 2.5 mM benzamidine, and 0.1 mM EDTA) were concentrated over a Diaflo PM-10 membrane (Amicon, Danvers, MA), made 20% (v/v) in glycerol, and stored at −90 °C. The FPGS preparation contained no detectable γ-glutamyl hydrolase activity;[33a] hydrolysis of <2% of the product synthesized in a standard FPGS assay would be detectable in this system.

Effects on L1210 FPGS. Results listed in Table VI were obtained as described in ref 29. The referenced methods are based on those reported in ref 33 and are similar to those summarized above (for human FPGS) except that specific activity measurements only were made for comparison. The concentrations of each substrate was 100 μM.

Acknowledgment. This investigation was supported by PHS Grants CA25236 (J.R.P.) CA18856 (F.M.S.), CA16056 (J.J.M.), CA22764 (F.M.S.), CA43500 (J.J.M.) from NCI, NIH, and AI30279 (J.R.P.) from NIAID, NIH. We thank Dr. Sherry F. Queener, Indiana University School of Medicine, for DHFR inhibition studies on **23b** and Dr. Elmer R. Pfefferkorn, Dartmouth Medical School, for *T. gondii* growth inhibition tests on **23b**.

References

(1) (a) Kisliuk, R. L. The Biochemistry of Folates. In *Folate Antagonists as Therapeutic Agents*; Sirotnak, F. M., Burchall, J. J., Ensminger, W. B., Montgomery, J. A., Eds.; Academic Press: Orlando, FL, 1984; Vol. 1, pp 1-68. (b) Jackson, R. C.; Grindey, G. B. The Biochemical Basis for Methotrexate Toxicity. In volume cited in ref 1a, pp 289–315.

(2) Blakley, R. L. Dihydrofolate Reductase. In *Folates and Pterins. Vol. 1. Chemistry and Biochemistry of Folates*; Blakley, R., Benkovic, S. J., Eds.; Wiley, New York, 1984; pp 191–253.

(3) Rosowsky, A. Chemistry and Biological Activity of Antifolates. In *Progress in Medicinal Chemistry*; Ellis, G. P.; West, G. B., Eds.; Elsevier Science Publishers, B. V. (Biomedical Division): New York, NY, 1989; Vol. 26, pp 1–252.

(4) Bertino, J. R. Ode to Methotrexate. *J. Clin. Oncol.* **1993**, *11*, 5–14.

(5) Schweitzer, B. I.; Dicker, A. P.; Bertino, J. R. Dihydrofolate Reductase as a Therapeutic Target. *FASEB J.* **1990**, *4*, 2441–2452.

(6) Prendergast, N. J.; Delcamp, T. J.; Smith, P. L.; Freisheim, J. H. Expression and Site-Directed Mutagenesis of Human Dihydrofolate Reductase. *Biochemistry* **1988**, *27*, 3664–3671.

(7) Davies, J. F. II; Delcamp, T. J.; Prendergast, N. J.; Ashford, V. A.; Freisheim, J. H.; Kraut, J. Crystal Structures of Recombinant Human Dihydrofolate Reductase Complexed with Folate and 5-Deazafolate. *Biochemistry* **1990**, *29*, 9467–9479.

(8) Bernstein, F. C.; Koetzle, T. F.; Williams, G. J. B.; Meyer, E. F.; Brice, M. D.; Rodgers, J. R.; Kennard, O.; Shimanouchi, T.; Tasumi, M. The Protein Databank: A Computer-based Archival File for Macromolecular Structures. *J. Mol. Biol.* **1977**, *112*, 535–542.

(9) Montgomery, J. A.; Piper, J. R.; Elliott, R. D.; Roberts, E. C.; Temple, C., Jr.; Shealy, Y. F. Derivatives of 2,4-Diamino-6-methylpteridine. *J. Heterocycl. Chem.* **1979**, *16*, 537–539.

(10) (a) Piper, J. R.; Montgomery, J. A. 6-(Bromomethyl)-2,4-diaminopteridine Hydrobromide. U.S. Pat. 4 077 957, 1978. (b) Piper, J. R.; Montgomery, J. A. Method of Making Pteridine Compounds. U. S. Pat. 4 079 056, 1978.

(11) Broughton, M. C.; Queener, S. F. *Pneumocystis carinii* Dihydrofolate Reductase Used To Screen Potential Antipneumocystis Drugs. *Antimicrob. Agents Chemother.* **1991**, *35*, 1348–1355.

(12) Bolin, J. T.; Filman, D. J.; Matthews, D. A.; Hamlin, R. C.; Kraut, J. Crystal Structures of *Escherichia coli* and *Lactobacillus casei* Dihydrofolate Reductase Refined at 1.7 Å Resolution. *J. Biol. Chem.* **1982**, *257*, 13650–13662.

(13) Schornagel, J. H.; Chang, P. K.; Sciarini, L. J.; Moroson, B. A.; Mini, E; Cashmore, A. R.; Bertino, J. R. Synthesis and Evaluation of 2,4-Diaminoquinazoline Antifolates with Activity Against Methotrexate-Resistant Human Tumor Cells. *Biochem. Pharmacol.* **1984**, *33*, 3251–3255.

(14) Ohemeng, K. A.; Roth, B. Receptor-Based Design of Novel Dihydrofolate Reductase Inhibitors: Benzimidazole and Indole Derivatives. *J. Med. Chem.* **1991**, *34*, 1383–1394.

(15) Nakayama, T.; Okutome, T.; Matsui, R.; Kurumi, M.; Sakurai, Y.; Aoyama, T.; Fujii, S. Synthesis and Structure-Activity Study of Protease Inhibitors. II. Amino- and Guanidino-Substituted Naphthoates and Tetrahydronaphthoates. *Chem. Pharm. Bull.* **1984**, *32*, 3968–3980.
(16) Leuck, G. J.; Perkins, R. P.; Whitmore, F. C. The Mercuration of Naphthalic Acids. *J. Am. Chem. Soc.* **1929**, *51*, 1831–1836.
(17) Ram, S.; Ehrenkaufer, R. E. Ammonium Formate in Organic Synthesis: A Versatile Agent in Catalytic Hydrogen Transfer Reductions. *Synthesis* **1988**, 91–95.
(18) Krishnamurthy, S. A Highly Efficient and General *N*-Monomethylation of Functionalized Primary Amines via Formylation-Borane: Methyl Sulfide Reduction. *Tetrahedron Lett.* **1982**, *23*, 3315–3318.
(19) (a) Piper, J. R.; Montgomery, J. A. A Convenient Synthesis of Aminopterin and Homologs via 6-(Bromomethyl)-2,4-diaminopteridine Hydrobromide. *J. Heterocycl. Chem.* **1974**, *11*, 279–280. (b) Piper, J. R.; Montgomery, J. A. Preparation of 6-(Bromomethyl)-2,4-pteridinediamine Hydrobromide and Its Use in Improved Syntheses of Methotrexate and Related Compounds. *J. Org. Chem.*, **1977**, *42*, 208–211.
(20) Piper, J. R.; Malik, N. D.; Rhee, M. S.; Galivan, J.; Sirotnak, F. M. Synthesis and Antifolate Evaluation of the 10-Propargyl Derivatives of 5-Deazafolic Acid, 5-Deazaaminopterin, and 5-Methyl-5-deazaaminopterin. *J. Med. Chem.* **1992**, *35*, 332–337.
(21) Su, T.-L.; Huang, J.-T.; Chou, T.-C.; Otter, G. M.; Sirotnak, F. M.; Watanabe, K. A. Chemical Synthesis and Biological Activities of 5-Deazaaminopterin Analogues Bearing Substituent(s) at the 5- and/or 7-Position. *J. Med. Chem.* **1988**, *31*, 1209–1215.
(22) Piper, J. R.; Johnson, C. A.; Otter, G. M.; Sirotnak, F. M. Synthesis and Antifolate Evaluation of 10-Ethyl-5-methyl-5,10-dideazaaminopterin and an Alternative Synthesis of 10-Ethyl-10-deazaaminopterin (Edatrexate). *J. Med. Chem.* **1992**, *35*, 3002–3006.
(23) (a) Davoll, J.; Johnson, A. M. Quinazoline Analogues of Folic Acid. *J. Chem. Soc. C* **1970**, 997–1002. (b) Hynes, J. B.; Tomazic, A.; Kumar, A.; Kumar, V. Inhibition of Human Dihydrofolate Reductase by 2,4-Diaminoquinazolines Bearing Simple Substituents on the Aromatic Ring. *J. Heterocycl. Chem.* **1991**, *28*, 1981–1986.
(24) Piper, J. R.; McCaleb, G. S.; Montgomery, J. A.; Kisliuk, R. L.; Gaumont, Y.; Sirotnak, F. M. Syntheses and Antifolate Activity of 5-Methyl-5-deaza Analogues of Aminopterin, Methotrexate, Folic Acid, and N^{10}-Methylfolic Acid. *J. Med. Chem.* **1986**, *29*, 1080–1087.
(25) Verheyden, J. P. H.; Moffatt, J. G. Halo Sugar Nucleosides. III. Reactions for the Chlorination and Bromination of Nucleoside Hydroxyl Groups. *J. Org. Chem.* **1972**, *37*, 2289–2299.
(26) Krenitsky, T. A.; Freeman, G. A.; Shaver, S. R.; Beacham, L. M. III; Hurlbert, S.; Cohn, N. K.; Elwell, L. P.; Selway, J. W. T. 3′-Amino-2′,3′-dideoxyribonucleosides of Some Pyrimidines: Synthesis and Biological Activities. *J. Med. Chem.* **1983**, *26*, 891–895.
(27) Wiley, G. A.; Hershkowitz, R. L.; Rein, B. M.; Chung, B. C. Studies in Organophosphorus Chemistry. I. Conversion of Alcohols and Phenols to Halides by Tertiary Phosphine Dihalides. *J. Am. Chem. Soc.* **1964**, *86*, 964-965.
(28) Ellard, J. A. Synthesis of Methotrexate. U. S. Pat. 4 080 325, 1978.
(29) (a) Sirotnak, F. M.; Schmid, F. A.; Otter, G. M.; Piper, J. R.; Montgomery, J. A. Structural Design, Biochemical Properties, and Evidence for Improved Therapeutic Activity of 5-Alkyl Derivatives of 5-Deazaaminopterin and 5-Deazamethotrexate Compared to Methotrexate in Murine Tumor Models. *Cancer Res.* **1988**, *48*, 5686–5691. (b) Rumberger, B. G.; Schmid, F. A.; Otter, G. M.; Sirotnak, F. M. Preferential Selection During Therapy *in vivo* by Edatrexate Compared to Methotrexate of Resistant L1210 Cell Variants with Decreased Folylpolyglutamate Synthetase Activity. *Cancer Commun.* **1990**, *2*, 305–310.
(30) Data provided by S. F. Queener; test procedures described in ref 11.
(31) Data provided by E. R. Pfefferkorn; test procedure reported in Pfefferkorn, E. R.; Pfefferkorn, L. C. The Biochemical Basis for Resistance to Adenine Arabinoside in a Mutant of *Toxoplasma gondii*. *J. Parasitol.* **1978**, *64*, 486-492.
(32) Reviewed by Berman, E. M.; Werbel, L. M. The Renewed Potential for Folate Antagonists in Contemporary Cancer Chemotherapy. *J. Med. Chem.* **1991**, *34*, 479–485.
(33) (a) McGuire, J. J.; Hsieh, P.; Coward, J. K.; Bertino, J. R. Enzymatic Synthesis of Folylpolyglutamates. Characterization of the Reaction and its Products. *J. Biol. Chem.* **1980**, *255*, 5776–5788. (b) Bolanowska, W. E.; Russell, C. A.; McGuire, J. J. Activation of Mammalian Folylpolyglutamate Synthetase by Sodium Bicarbonate. *Arch. Biochem. Biophys.* **1990**, *281*, 198–203. (c) Segel, I. W. In *Enzyme Kinetics;* Wiley: New York, 1975.
(34) Mohamadi, F.; Richards, N. G.; Guida, W. C.; Liskamp, R.; Lipton, M.; Caufield, C.; Chang, G.; Hendrickson, T.; Still, W. C. MacroModel-An Integrated Software System for Modeling Organic and Bioorganic Molecules Using Molecular Mechanics. *J. Comput. Chem.* **1990**, *11*, 440–467.
(35) SYBYL Version 5.41. Tripos Associates, Inc., A Subsidiary of Evans and Sutherland, 1699 S. Hanley Rd., Suite 303, St. Louis, MO 63144.
(36) Weiner, S. J.; Kollman, P. A.; Case, D. A.; Singh, U. C.; Ghio, C.; Alagona, G.; Profeta, S.; Weiner, P. A New Force Field for Molecular Mechanical Simulation of Nucleic Acids and Proteins. *J. Am. Chem. Soc.* **1984**, *106*, 765–784.
(37) Still, W. C.; Tempczyk, A.; Hawley, R. C.; Hendrickson, T. A Semianalytical Treatment of Solvation for Molecular Mechanics and Dynamics. *J. Am. Chem. Soc.* **1990**, *112*, 6127–6129.
(38) Saunders, M.; Houk, K. N.; Wu, Y.-D.; Still, W. C.; Lipton, M.; Chang, G.; Guida, W. C. Conformations of Cycloheptadecane. A Comparison of Methods for Conformational Searching. *J. Am. Chem. Soc.* **1990**, *112*, 1419-1427.
(39) BATCHMIN is the non-interactive modeling program used in conjunction with MACROMODEL; see ref 34.
(40) Cohen, N. C.; Blaney, J. M.; Humblet, C.; Gund, P.; Barry, D. C. Molecular Modeling Software and Methods for Medicinal Chemistry. *J. Med. Chem.* **1990**, *33*, 883–894.